Arabian Journal of Chemistry (2016) 9, S466–S474

King Saud University

Arabian Journal of Chemistry

www.ksu.edu.sa
www.sciencedirect.com

ORIGINAL ARTICLE

A new alternative adsorbent for the removal of cationic dyes from aqueous solution

T. Santhi [a,*], S. Manonmani [b], V.S. Vasantha [c], Y.T. Chang [d]

[a] Department of Chemistry, Karpagam University, Coimbatore 641021, India
[b] Department of Chemistry, PSG College of Arts and Science, Coimbatore 641014, India
[c] Department of Natural Product Chemistry, Madurai Kamaraj University, Madurai 625021, India
[d] Department of Chemical and Materials Engineering, Nanya Institute Technology, Jhongli 32091, Taiwan

Received 25 February 2011; accepted 6 June 2011
Available online 22 June 2011

KEYWORDS

Adsorption;
Annona squmosa seed;
Methylene blue;
Malachite green

Abstract Adsorption of Malachite green (MG) and Methylene blue (MB) from aqueous solutions on low cost adsorbent prepared from *Annona squmosa* seed (CAS) is studied experimentally. Results obtained indicate that the removal efficiency of Malachite green and Methylene blue at 27 ± 2 °C exceeds 75.66% and 24.33% respectively, and that the adsorption process is highly pH-dependent. Results showed that the optimum pH for dye removal is 6.0. The amount of dye adsorbed from aqueous solution increases with the increase of the initial dye concentration. Smaller adsorbent particle adds to increase the percentage removal of Malachite green and Methylene blue. The equilibrium data fitted well to the Langmuir model ($R^2 > 0.97$) and the adsorption kinetic followed the pseudo-second-order equation ($R^2 > 0.99$). The maximum adsorption capacities of MG, MB on CAS are 25.91 mg g^{-1} and 08.52 mg g^{-1} respectively. These results suggest that *A. squmosa* seed is a potential low-cost adsorbent for the dye removal from industrial wastewater. The adsorption capacity of CAS on MG is greater than MB.

1. Introduction

More than 10,000 dyes have been widely used in textile, paper, rubber, plastics, leather, cosmetic, pharmaceutical, and food industries, which generated huge volume of wastewater every year (Mondal, 2008). The disposal of dye wastewater without proper treatment is a big challenge and has caused harm to the aquatic environment, such as reducing light penetration and photosynthesis (Garcia-Montano et al., 2008). Some of dyes contained in wastewater even decompose into carcinogenic aromatic amines under anaerobic conditions, which could cause serious health problems to humans and animals (Chen et al., 2003). Due to the complex molecular structure, dyes are usually very difficult to be biodegraded, making them hardly eliminated under natural aquatic environment (Kar et al., 2009).

Due to the low biodegradability, conventional biological wastewater treatment processes are not efficient in treating

* Corresponding author. Tel.: +91 9965535701.
E-mail address: ssnilasri@yahoo.co.in (T. Santhi).
Peer review under responsibility of King Saud University.

ELSEVIER Production and hosting by Elsevier

http://dx.doi.org/10.1016/j.arabjc.2011.06.004

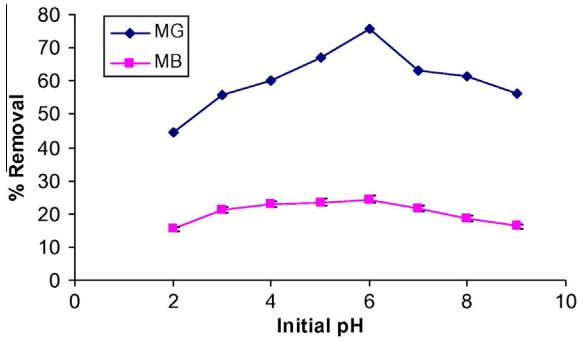

Figure 1 Effect of pH on the removal of MG and MB onto CAS (CAS dosage 200 mg/50mL, MG 100 mg/L).

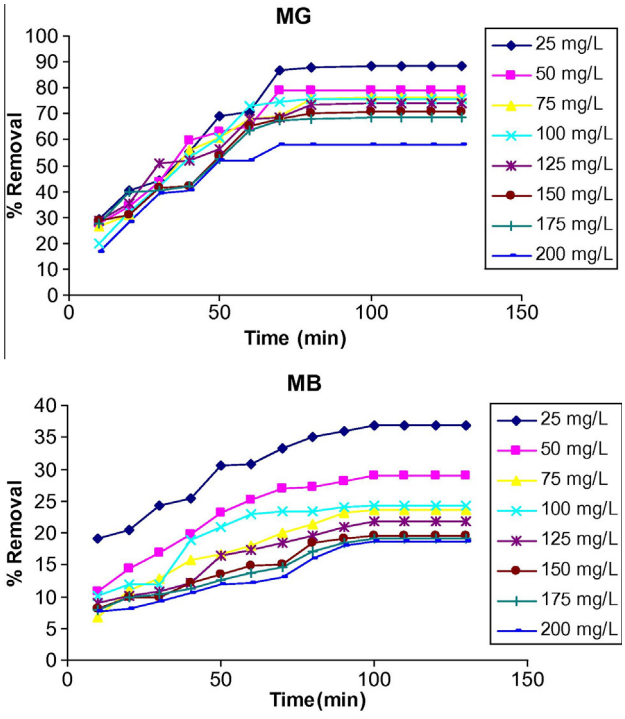

Figure 2 Effect of contact time on the removal of different initial concentrations of MG and MB using CAS (0.2 g/50 mL) at pH 6.0.

dyes wastewater (Mondal, 2008). Therefore, dye wastewater are usually treated by physical and/or chemical methods, such as coagulation and flocculation (Zonoozi et al., 2009), membrane separation (Sachdeva and Kumar, 2009), activated carbon adsorption (Tan et al., 2008), electrochemical removal, and photochemical degradation. However, for the developing countries, these methods are still too expensive to be used widely. Developing economical adsorbents to treat dye wastewater has attracted great interest in recent years (Kavitha and Namasivayam, 2007). Gupta and Suhas (2009) recently reviewed the application of low-cost adsorbents for the dye removal.

Annona squmosa is a commonly available hedge plant, which is used in fencing property perimeter in Kenerapallam, Palaghat Dt, Kerala. Foliage of the plant is thick and fruits are in abundance during the session. The inner core of the ripe fruit is delicious and of nutritive value and commonly consumable. After consumption, the seeds are discarded as they are nonedible. Since the *A. squmosa* seed is available free of cost, only the carbonization of it is involved for the waste water treatment. Therefore the main objective of this study was to evaluate the possibility of using dried *A. squmosa* seed to develop a new low-cost activated carbon and study its application to remove malachite green and Methylene blue from simulated wastewater. Systematic evaluation of the parameters involved, such as pH, adsorbent dose, adsorbent particle size, initial dye concentration and time was undertaken.

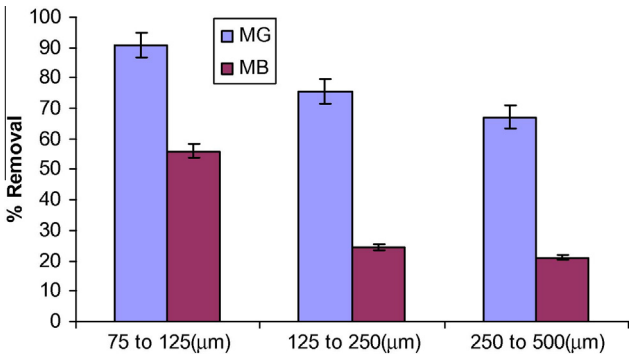

Figure 3 Effect of adsorbent particle size on MG and MB removals (C_0: 100 mg L^{-1}, pH 6.0, agitation speed: 150 rpm, temperature: 27 ± 2 °C).

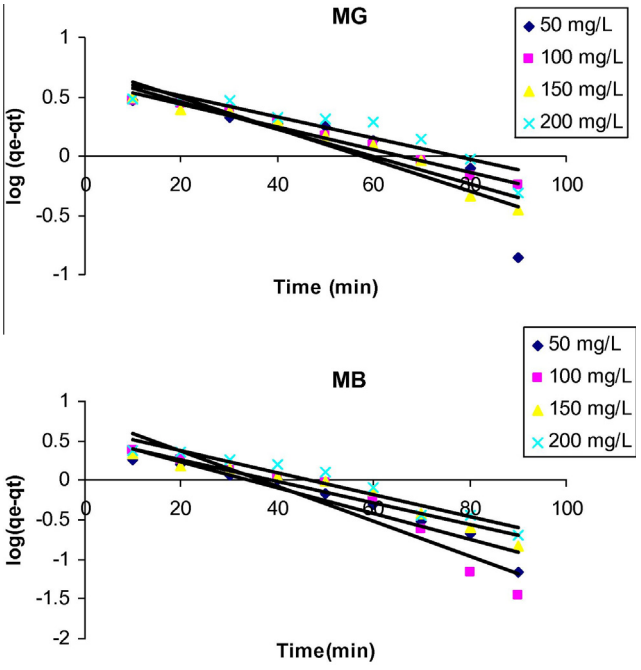

Figure 4 Pseudo-first-order kinetics for MG and MB adsorption onto CAS. Conditions: adsorbent dosage 0.2 g/50 mL, pH 6.0, temperature 27 ± 2 °C.

Table 1 Comparison of the Lagergrens first-order kinetic model and pseudo second order kinetic model rate constants, different initial MG and MB concentration onto CAS (0.2 g/50 mL).

	Co (mg/L)	q_e (exp) (mg/g)	Pseudo-first-order			Pseudo-second-order			
			K_1 (min)	q_e (cal) mg/g	R^2	K_2 (g/mg min)	q_e (cal) mg/g	h (mg/g min)	R^2
MG	50	09.9038	0.0302	5.6493	0.9920	0.0091	10.5374	1.0080	0.9934
	100	18.9150	0.0219	4.2864	0.9930	0.0120	19.2678	4.4464	0.9965
	150	26.4675	0.0269	4.9226	0.9850	0.0122	26.9542	8.8731	0.9996
	200	29.0550	0.0207	4.8640	0.9609	0.0106	29.4118	9.1827	0.9995
MB	50	03.6238	0.0373	3.5859	0.9269	0.0113	4.2937	0.2077	0.9889
	100	06.0825	0.0511	6.4953	0.8940	0.0121	6.7889	0.5572	0.9948
	150	07.3725	0.0316	3.4689	0.9388	0.0161	7.80031	0.9761	0.9957
	200	09.3700	0.0320	4.4998	0.9347	0.0118	9.9701	1.1773	0.9947

2. Materials and methods

2.1. Adsorbent (CAS)

A. squmosa seed was thoroughly washed with tap water to remove dirt and grime then rinsed a few times with distilled water and air-dried. *A*. *squmosa* seed was dried, ground and sieved to different particle sizes and preserved in desiccator until use.

Chemical activation using H_2SO_4 at moderate temperatures produces a high surface area and high degree of micro-porosity. The dried biomass (1.0 kg) was added to 1000 mL of 98% H_2SO_4 and kept for 12 h at room temperature, washed thoroughly with distilled water until it attained the neutral pH and soaked in 2% $NaHCO_3$ solution overnight in order to remove any excess acid present. The material was then washed with distilled water until it reached neutral pH and dried at 110 ± 2 °C. The dry carbon was crushed into granules, sieved to different particle sizes and then preserved in desiccator until use.

Scanning electron microscopy (SEM) (Philips 501), BET (a continuous flow Nelson Eggertson type surface area analyzer), X-ray diffraction (XRD) (Arhensdurg Germany (Model No. ID 3000)), Elemental analysis was carried out with a C.H.N. 1106 Carlo Erba MicroAnalysing device equipped with inductive furnace analyzer and FT-IR spectra (Shimadzu, Model FTIR-8201PC) analysis was carried out on the CAS to study its surface texture and functional groups responsible for the adsorption of dyes.

2.2. Adsorbate

A stock solution of 500 mg/L was prepared by dissolving the appropriate amount of Malachite green (MG) and Methylene blue (MB) (obtained from S.D. Fine Chemicals, Mumbai, India) in 1000 mL with distilled water. Different concentrations ranged between 25 and 200 mg/L of MG and MB were prepared from the stock solution. All the chemicals used throughout this study were of analytical-grade reagents. Double-distilled water was used for preparing all of the solutions and reagents. The initial pH is adjusted with 0.1 M HCl or 0.1 M NaOH. All the adsorption experiments were carried out at room temperature (27 ± 2 °C).

2.3. Batch adsorption studies

Batch experiments were conducted to investigate the parametric effects of pH, adsorbent particle size, adsorbent dose, initial adsorbate concentration and adsorption time for MG and MB adsorption on the prepared carbon. Dye samples were prepared by dissolving a known quantity in distilled water and used as a stock solution and diluted to the required initial concentration (range: 25–200 mg/L). Batch adsorption experiments were carried out in a rotary shaker at 150 rpm using 250 mL shaking flasks at room temperature. The adsorbent and adsorbate solutions were separated by centrifuging at 3000 rpm for 5 min. The concentration of dye in solution was measured by using Systronic UV–vis Spectrophotometer-104. All the experiments were duplicated and only the mean values are reported. The maximum deviation observed was less than ± 4%.

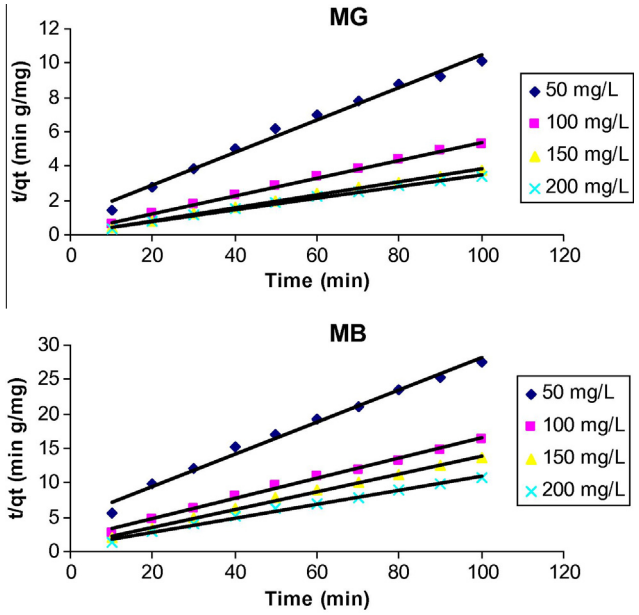

Figure 5 Pseudo-second- order kinetics for MG and MB adsorption onto CAS. Conditions: adsorbent dosage 0.2 g/ 50 mL, pH 760, temperature 27 ± 2 °C.

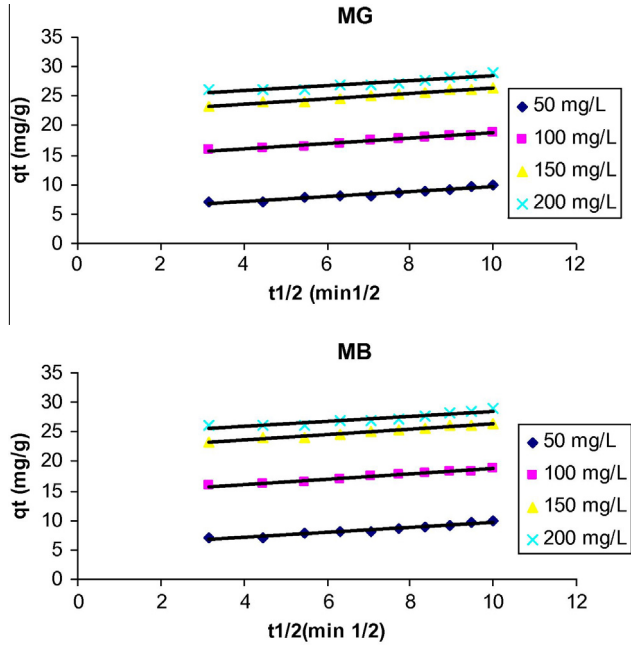

Figure 6 Intraparticle diffusion plot for MG and MB adsorption onto CAS. Conditions: adsorbent dosage 0.2 g/50 mL, pH 6.0, temperature 27 ± 2 °C.

The amount of dye adsorbed at equilibrium onto carbon, q_e (mg/g), was calculated by the following mass balance relationship:

$$q_e = (C_0 - C_e)V/W \quad (1)$$

where C_0 and C_e (mg/L) are the initial and equilibrium liquid-phase concentration of dyes, respectively, V the volume of the solution (L), and W is the weight of the carbon used (g).

For kinetic studies, 200 mg of CAS was contacted with 50, 100, 150 and 200 mg/L dye solution (50 mL) using a shaker at 150 rpm at room temperature. At predetermined time intervals, the amount of uptake of dye was evaluated spectrophoto metrically.

3. Results and discussion

3.1. Effect of pH

pH is one of the most important factors affecting the adsorption process. In order to investigate the influence of pH on the MG and MB removal by CAS, experiments were carried out over a pH range of 2.0–9.0 at dye concentration 50 mg/ L, adsorbent dosage 0.2 g/50 mL. As shown in Fig. 1, the maximum removal efficiency, approximately 75.66% for MG and 24.33% for MB were achieved around pH 6.0.

Several parameters such as adsorption capacity of adsorbent, surface charges and active sites might be attributed to the adsorption behavior of the adsorbent at various pHs. The surface of CAS contains a large number of active sites. The dye uptake can be related to the active sites and also to the chemistry of the dye in the solution. Theoretically, at pH < isoelectrical point, the surface gets positively charged, which enhances the adsorption of the negatively charged dye anions through electrostatic forces of attraction. At pH > isoelectrical point, the surface of CAS particles gets negatively charged, which favors the adsorption of cationic dye (Ahmad and Kumar, 2010). As the pH of dye solution becomes higher, the association of dye cations with negatively charged functional groups in the adsorbent surface could more easily take place as follows:

$$S\text{–}OH + OH^- \rightarrow SO^- + H_2O \quad (12)$$

$$SO^- + Dye^+ \rightarrow S - O - Dye \quad (13)$$

3.2. Effect of adsorbate concentrations and equilibrium time

The removal of MG and MB by adsorption on CAS was found to increase with time and attained a maximum value at 100 min (Fig. 2). On changing the initial concentration of MG and MB solution from 25 to 200 mg/L, the amount adsorbed increased from 5.5356 to 29.0550 mg/g and percentage removal decreased from 88.57 to 58.11 with increased concentration of dye from 25 to 200 mg/L for MG and the amount adsorbed increased from 2.3075 to 9.3700 mg/g and percentage removal decreased from 36.92 to 18.74 with increased concentration of dye from 25 to 200 mg/L for MB .

This may be due to the fact that at lower concentrations almost all the dye molecules were adsorbed very quickly on the outer surface, but further increase in initial dye concentrations led to fast saturation of adsorbent surface, and thus most of the dye adsorption took place slowly inside the pores (Hameed and EI-Khaiary, 2008).

3.3. Effect of adsorbent particle size

The batch adsorption experiments were carried out using adsorbent with different particle sizes (75–125 μm to 250–500 μm) at pH 6.0, and initial concentration of 100 mg/L. The removal of

Table 2 The parameters obtained from intraparticle diffusion model using different initial MG and MB concentrations onto CAS (0.2 g/50 mL).

Adsorbents	C_0 (mg L^{-1})	K_{dif}	C	R^2
MG	50	0.181	5.4657	0.9482
	100	0.3856	7.4605	0.9510
	150	0.454	21.808	0.9820
	200	0.4527	24.054	0.9027
MB	50	0.2805	0.9028	0.9897
	100	0.3618	2.6631	0.9827
	150	0.3044	4.3525	0.9854
	200	0.3845	5.5365	0.9695

Table 3 Comparison of the coefficients isotherm parameters for MG and MB adsorption onto CAS.

Isotherm model	Adsorbate	
	MG	MB
Langmuir		
Q_m (mg g^{-1})	25.91	08.53
K_a (L mg^{-1})	0.155	0.035
R^2	0.9702	0.9701
Freundlich		
$1/n$	0.4916	0.3695
K_f (mg g^{-1})	3.7880	1.1863
R^2	0.9039	0.8759
Dubinin–Radushkevich		
Q_m (mg g^{-1})	25.279	06.785
K ($\times 10^{-5}$ mol^2 kJ^{-2})	0.11	0.03
E (kJ mol^{-1})	0.2673	0.1289
R^2	0.8801	0.9214

MG and MB increased with the decrease in particle size (Fig. 3). The relatively higher adsorption with smaller adsorbent particle may be attributed to the fact that smaller particles yield large surface areas (Liew Abdullah et al., 2005).

3.4. Adsorption dynamics

Lagergren's pseudo-order equation is widely used to investigate the dynamics of the adsorption process from aqueous solution (Allen et al., 2005). In this study, pseudo-first-order equation and pseudo-second-order equation were separately used to describe the adsorption process of MG and MB onto CAS.

Log $(q_e - q)$ was calculated using the first-order Lagergren equation, as shown in Eq. (2).

$$\log(q_e - q) = \log q_e - \frac{k_{ad}}{2.303} t \tag{2}$$

where k_{ad} is the rate constant of first-order adsorption (min^{-1}), q_e and q are the amounts of dye adsorbed on adsorbent at equilibrium and at time t (min), respectively. A plot of log $(q_e - q)$ versus t is shown in Fig. 4, in which the shape of the lines indicates that the first-order Lagergren equation did not fit well to the whole range of the adsorption process and was generally applicable over the initial stage of the contact time (Vimonses et al., 2009). Therefore, the second-order Lagergren equation was also applied to describe the adsorption process, as listed in Eqs. (3) and (4).

$$\frac{t}{q} = \frac{1}{k_2 q_e^2} + \frac{1}{q_e} \tag{3}$$

and

$$h = k_2 q_e^2 \tag{4}$$

where k_2 is the pseudo-second-order rate constant (g mg^{-1} min^{-1}) and h is the initial adsorption rate at time approaching 0 (mg g^{-1} min^{-1}). The intercept of the plots of t/q versus t was used to calculate the rate constant k_2 and the initial adsorption rate h. Table 1 lists the values of the rate constant k_2, the initial adsorption rate h and the regression coefficient R^2. All regression coefficients were more than 0.99 and the pseudo-second-order equation fitted very well to the adsorption. As seen in Fig. 5, the pseudo-second-order equation is more likely to predict the behavior over the whole range of the adsorption process. Furthermore, the correlation coefficients R^2 for the pseudo first order kinetic model obtained for all concentrations of dyes are lower than the R^2 for pseudo second order kinetic model (Table 1), and the predicted q_e values deviated reasonably from the experimental values (Table 1). This shows that the adsorption of MG and MB onto CAS did not obey the pseudo first-order model of Lagergren.The effect of intraparticle diffusion resistance on adsorption was evaluated by intraparticle diffusion model to identify the adsorption mechanism (Alkan et al., 2004; Chiou and Li, 2003), as expressed in Eq. (4).

Table 4a Comparison of adsorption capacities with other low cost adsorbent for MG.

Adsorbent	q_m (mg g^{-1})	References
Hen feather	10.30	Mittal (2006)
Bentonite	7.72	
Rubber wood Sawdust	25.80	Kumar and Sivanesan (2007)
Activated charcoal	00.17	Iqbal and Ashiq (2007)
Lemon peel	03.20	Kumar and Vasanth (2007)
Activated charcoal	00.18	Iqbal and Ashiq (2007)
Arundo donax root carbon	08.69	Zhang et al. (2008)
Maize cob	11.89	Sonawane and Shrivastava (2009)
Neem saw dust	04.23	Khattri and Singh (2009)
Coffee bean	24.80	Baek et al. (2010)
Luffa cylindrical	21.60	Altinisik et al. (2010)
A. squmosa (CAS)	25.91	This study

Table 4b Comparison of adsorption capacities with other low cost adsorbent for MB.

Adsorbent	q_m (mg g^{-1})	References
Raw beech sawdust	09.78	Batzias and Sidiras (2004)
Neem leaf powder	08.76	Bhattacharyya and Sharma (2005)
Glass wool	02.25	Chakrabarti and Dutta (2005)
Fly ash	02.63	Rao and Rao (2006)
Coir pith carbon	05.87	Kavitha and Namasivayam, 2007
Posidonia oceanica L fibers	05.56	Cibi et al. (2007)
Petrified sediment	02.04	Aroguz et al. (2008)
Caulerpa racemosa varcylindracea	03.42	Cengiz and Cavas (2008)
A. squmosa (CAS)	08.52	This study

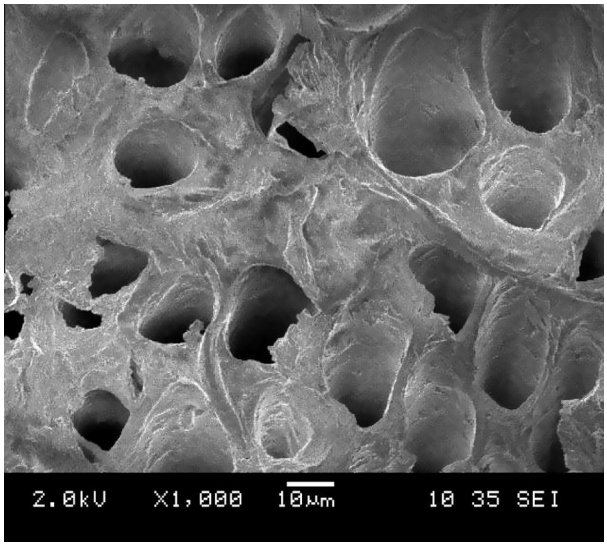

Figure 7 SEM photographs for CAS (2.0 ku × 1000).

$$q = k_{id} t^{1/2} + I \quad (5)$$

where k_{id} is the rate constant of intraparticle diffusion (mg g^{-1} min$^{-0.5}$). Values of I give the information regarding the thickness of boundary layer.

The values of q_t were found to be linearly correlated with values of $t^{1/2}$ (Fig 6) and the rate constant K_{dif} directly evaluated from the slope of the regression line (Table 2). The values of intercept C (Table 2) provide information about the thickness of the boundary layer, the resistance to the external mass transfer increase as the intercept increase. The constant C was found to increase with increase of dye concentration from 50 to 200 mg L^{-1}, which indicating the increase of the thickness of the boundary layer and decrease of the chance of the external mass transfer and hence increase of the chance of internal mass transfer. The R^2 values given in Table 2 are close to unity indicating the application of this model. This may confirm that the rate-limiting step is the intraparticle diffusion process. The linearity of the plots demonstrated that intraparticle diffusion played a significant role in the uptake of the adsorbate by adsorbent. However, as still there is no sufficient indication about it, Ho (2003) has shown that if the intraparticle diffusion is the sole rate-limiting step, it is essential for the q_t versus $t^{1/2}$ plots to pass through the origin, which is not the case in Fig. 6, it may be concluded that surface adsorption and intraparticle diffusion were concurrently operating during the dye and CAS interactions.

3.5. Adsorption isotherm

Langmuir isotherm models have been applied to describe the adsorption of dyes by different materials (Vimonses et al., 2009). In this study, the values of $C_e q_e^{-1}$ and C_e were calculated using Eq. (8).

$$\frac{C_e}{q_e} = \frac{1}{Q^0 b} + \frac{C_e}{Q^0} \quad (6)$$

where Q^0 is the maximum adsorption capacity of CAS (mg g^{-1}) and b is the equilibrium constant related to the adsorption energy (L mg^{-1}). The linear plots of $C_e q_e^{-1}$ versus C_e showed that the adsorption followed a Langmuir isotherm, as shown in Table 3 ($R^2 > 0.98$). The Q^0 and b were determined from the slopes and intercepts of the respective plots and are listed in Table 3. The maximum adsorption capacities on the adsorption of MG by CAS was 25.91 mg g^{-1}, MB by CAS was 8.53 mg g^{-1}.

The Freundlich isotherm model can be used for non-ideal sorption that involves heterogeneous adsorption. The Freundlich isotherm can be derived assuming a logarithmic decrease in the enthalpy of adsorption with the increase in the fraction of occupied sites and is commonly given by the following non-linear equation:

$$q_e = K_F C_e^{1/n} \quad (7)$$

where K_F can be defined as the adsorption or distribution coefficient and represents the quantity of dye adsorbed onto adsorbent for unit equilibrium concentration. $1/n$ is indicating the adsorption intensity of dye onto the adsorbent or surface heterogeneity, becoming more heterogeneous as its value gets closer to zero. A value for $1/n$ below 1 indicates concurrence with Langmuir isotherm while $1/n$ above 1 indicates a cooperative adsorption between Langmuir and Freundlich adsorption isotherm. The correlation coefficients (R^2) values were higher than 0.9000, however, the R^2 values for the Langmuir equation for MG and MB are higher than those obtained for the Freundlich equation (Table 3). The constant $1/n$ is lower than 1.0, indicating that MG and MB are favorably adsorbed by the adsorbents (Ponnusami et al., 2008).

The D–R isotherm dose not assumes a homogeneous surface or constant adsorption potential. The D–R model has commonly been applied as

$$q_e = Q_m \exp(-K\varepsilon^2) \quad (8)$$

$$\ln q_e = \ln Q_m - K\varepsilon^2 \quad (9)$$

where K is a constant related to the adsorption energy, Q_m the theoretical saturation capacity, ε the Polanyi potential, calculated from Eq. (10).

$$\varepsilon = RT \ln\left(1 + \frac{1}{C_e}\right) \quad (10)$$

The mean free energy of adsorption (E), defined as the free energy change when one mole of ion is transferred from infinity in solution to the surface of the solid, was calculated from the K value using the following relation

$$E = \frac{1}{\sqrt{2K}} \quad (11)$$

The calculated value of D–R parameters is given in Table 3. The saturation adsorption capacity Q_m obtained using the D–R isotherm model for adsorption of dyes onto the adsorbents used in this study is close to that obtained from the Langmuir isotherm model (Table 3). The values of E calculated using Eq. (11) is below 20 kJ mol^{-1} for MG and MB indicating that the physico-sorption process plays the significant role in the adsorption of dyes onto adsorbents (Bulut et al., 2008b). The E values are below 16 kJ mol^{-1} for MG and MB adsorption onto CAS indicates that the adsorption type may be physical or ion exchange (Altinisik et al., 2010).

3.6. Comparison of various low cost adsorbents

Tables 4a and 4b compares the adsorption capacity of different types of adsorbents used for removal of MG and MB. The most important parameter to compare is the Langmuir Q_m value since it is a measure of adsorption capacity of the adsorbent. The value of Q_m in this study is larger than those in most of previous works. This suggests that MG, MB could be easily adsorbed on CAS.

3.7. Characterization of CAS (SEM, BET and FTIR of CAS)

The surface structure of CAS was analyzed by scanning electronic microscopy (SEM) (Fig. 7 It is clear that the adsorbents have considerable number of heterogeneous pores, a cave- like, uneven and rough surface morphology, where there is a good possibility for dye to be trapped and adsorbed (Hameed and EI-Khaiary, 2008).

The adsorbents have heterogeneous surface, micro pores and mesopores as seen from its surface micrographs. The reported Brunauer–Emmett–Teeller (BET) surface area of the adsorbents is 20.54 m^2/g for CAS.

The FTIR spectrum of CAS shows distinct peaks at 3922–3445 cm^{-1} (OH stretch), 2928.47 cm^{-1} (CH stretch shift), 2361, 2341, 2290 cm^{-1} (NH stretch), 1747.36 cm^{-1} (C═O stretch disappeared), 1498 cm^{-1} (phenyl), and 1020 cm^{-1} (C–O–C stretch), It is clear that the adsorbent displays a number of adsorption peaks, reflecting the complex nature of the adsorbent.

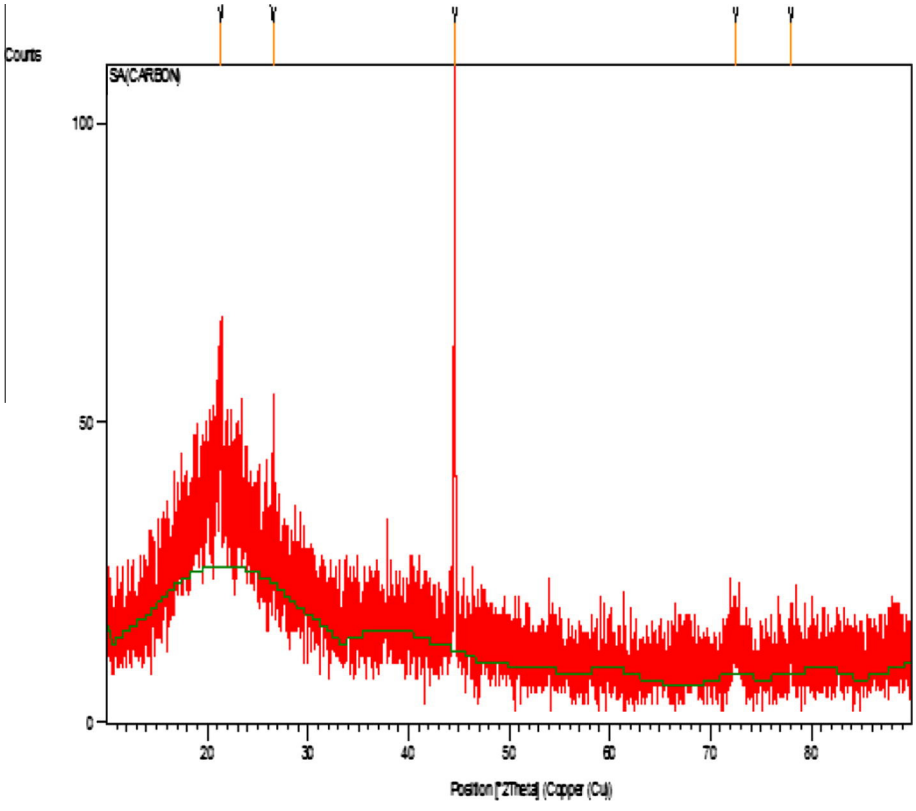

Figure 8 XRD photograph for CAS.

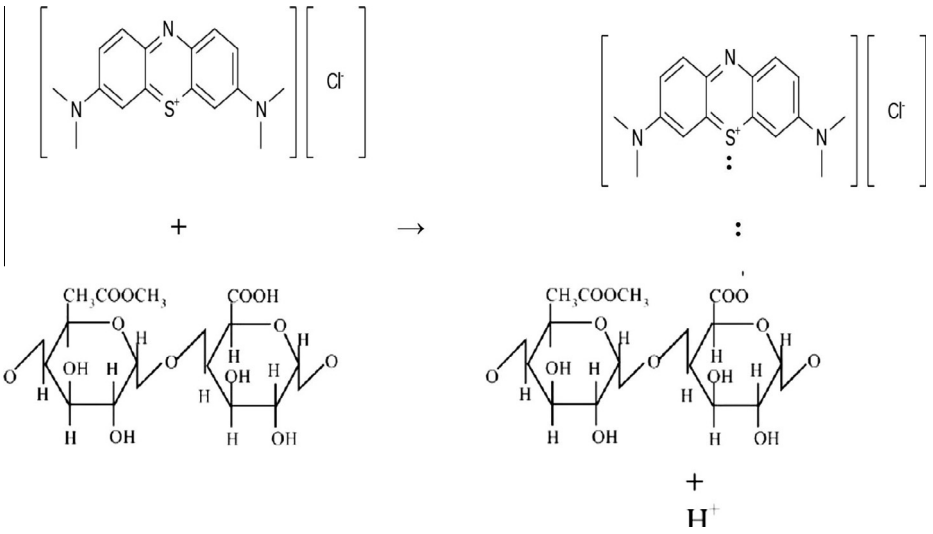

The adsorbents can be crystallographically characterized by means of X-ray diffraction (XRD). The XRD pattern (Fig. 8) of the adsorbents show typical spectrum having main and secondary peaks at 2Θ of 22° and 37° respectively. The main peak is taken as indicative of the presence of highly organized crystalline cellulose while the secondary peak is a measure of polysaccharides structure (Sonawane and Shrivastava, 2009). The results showed that the adsorbents have more pores and crystalline structure. The availability of more surface area is due to the typical lateral rack type of structure of the adsorbents as was clearly witnessed in the SEM micrographs.

The percentages of total carbon, nitrogen and hydrogen in CAS are 49.11, 06.11, and 01.12 which shows that the adsorbents contain mainly carbon with less amounts of nitrogen and hydrogen. A relatively larger percentage of carbon and hydrogen in comparison to nitrogen compounds indicates that carbon-hydrogen groups might be available for adsorption of dyes (Sonawane and Shrivastava, 2009).

3.8. Adsorption mechanism

Activated carbons are materials which have amphoteric characteristics, so the pH on its surface always changes depending on initial pH of the solution. Generally, the adsorption capacity and rate constant have the tendency to increase as initial pH of the solution increases. This is due to the pH_{zpc} of the adsorbents which has an acidic value, this is favorable for cation adsorption (Prahas et al., 2008). The FTIR spectrum of the adsorbent indicates that carboxyl and hydroxyl groups are present in abundance. The sorption of MB on the adsorbent may be due to the electrostatic attraction between these groups and the cationic dye molecules (MG^+). At pH above 4, the carboxylic groups are deprotonated and negatively charged carboxylate ligands (–COO–) bind to the positively charged MG, MB molecules. This confirms that the sorption of MG and MB by adsorbent was an ion exchange mechanism between the negatively charged groups present in adsorbent and the cationic dye molecule (Saeed et al., 2010). These positively charged ions in the presence of dye solution could then be exchanged with dye cations as follows.

4. Conclusions

This study investigated the removal of MG and MB by CAS from aqueous solution. The removal efficiency of MG and MB decreased with increasing adsorbate concentration. The equilibrium time was about 100 min. The removal efficiency was dependent of pH. Adsorption dynamics analysis indicates that pseudo-second-order equation fitted very well to the adsorption of MG, MB on CAS ($R^2 > 0.99$). Intraparticle diffusion model shows that more than one mode of diffusion functioned in the adsorption of MG, MB on CAS. The adsorption process followed well to the Langmuir model ($R^2 > 0.97$). The maximum adsorption capacities on the adsorption of MG by CAS was 25.91 mg g^{-1}, MB by CAS was 8.53 mg g^{-1}. These results suggest that CAS is a potential low-cost adsorbent for the dye removal from industrial wastewater.

References

Ahmad, R., Kumar, R., 2010. Adsorption studies of hazardous malachite green onto treated ginger waste. J. Environ. Manage. 91, 1032–1038.

Alkan, M., Demirbas, O., Celikcapa, S., Dogan, M., 2004. Sorption of Acid Red 57 from aqueous solution onto sepiolite. J. Hazard. Mater. 116, 135–145.

Allen, S.J., Gan, Q., Matthews, R., Johnson, P.A., 2005. Kinetic modeling of the adsorption of basic dyes by kudzu. J. Colloid Interf. Sci. 286, 101–109.

Altinisik, A., Gur, E., Seki, Y., 2010. A natural sorbent, Luffa cylindrical for the removal of a model basic dye. J. Hazard. Mater. 179, 658–664.

Aroguz, A.Z., Gulen, J., Evers, G.H., 2008. Adsorption of methylene blue from aqueous solution on pyrolysed petrified sediment. Bioresour. Technol. 99, 1503–1508.

Baek, M.H., Ijagbemi, C.O., Jin, O.S., Su Kim, D., 2010. Removal of malachite green from aqueous solution using degreased coffee bean. J. Hazard. Mater. 176, 820–828.

Batzias, F.A., Sidiras, D.K., 2004. Dye adsorption by calcium chloride treated beech sawdust in batch and fixed bed systems. J. Hazard. Mater. B114, 167–174.

Bhattacharyya, K.G., Sharma, A., 2005. Kinetics and thermodynamics of methylene blue adsorption on neem (*Azadirachta indica*) leaf powder. Dyes Pig. 65, 51–59.

Bulut, E., Ozacar, M., Ayhan Sengil, I., 2008b. Adsorption of malachite green onto bentonite: Equilibrium and kinetic studies and process design. Micropor. Mesopor. Mater. 115, 234–246.

Cengiz, S., Cavas, L., 2008. Removal of methylene blue by invasive marine sea weed: Caulerpa racemosavar Cylindracea. Bioresour. Technol. 99, 2938–2946.

Chakrabarti, S., Dutta, B.K., 2005. Note on the adsorption and diffusion of methylene blue in glass fibers. J.Colloid Interf. Sci. 286, 807–811.

Chen, K.C., Wu, J.Y., Yang, W.B., Hwang, S.C.J., 2003. Evaluation of effective diffusion coefficient and intrinsic kinetic parameters on azo dye biodegradation using PVA-immobilized cell beads. Biotechnol. Bioeng. 83, 821–832.

Chiou, M.S., Li, H.Y., 2003. Adsorption behavior of reactive dye in aqueous solution on chemical cross-linked chitosan beads. Chemosphere 50, 1095–1105.

Cibi, M.C., Mahjoub, B., Seffen, M., 2007. Kinetic and equilibrium studies of methylene blue biosorption by Posidonia oceanica (L) fibres. J. Hazard. Mater. B139, 280–285.

Garcia-Montano, J., Torrades, F., Perez-Estrada, L.A., Oller, I., Malato, S., Maldonado, M.I., Peral, J., 2008. Degradation pathways of the commercial reactive azo dye Procion Red H-E7B under solar-assisted photo-Fenton reaction. Environ. Sci. Technol. 42, 6663–6670.

Hameed, B.H., EI-Khaiary, M.I., 2008. Removal of basic dye from aqueous medium using a novel agricultural waste material: Pumpkin seed hull. J. Hazard. Mater. 155, 601–609.

Ho, Y.S., 2003. Removal of copper ions from aqueous solution by tree fern. Water Res. 37, 2323–2330.

Iqbal, M.J., Ashiq, M.N., 2007. Adsorption of dyes from aqueous solutions on activated charcoal. J. Hazard. Mater. B139, 57–66.

Kar, A., Smith, Y.R., Subramanian, V., 2009. Improved photocatalytic degradation of textile dye using titanium dioxide nanotubes formed over titanium wires. Environ. Sci. Technol. 43, 3260–3265.

Kavitha, D., Namasivayam, C., 2007. Experimental and kinetic studies on methylene blue adsorption by coir pith carbon. Bioresour. Technol. 98, 14–21.

Khattri, S.D., Singh, M.K., 2009. Removal of malachite green from dye wastewater using neem sawdust by adsorption. J. Hazard. Mater. 167, 1089–1094.

Kumar, K.V., Sivanesan, S., 2007. Isotherms for Malachite Green onto rubber wood (Hevea brasiliensis) sawdust: comparison of linear and non-linear methods. Dyes Pig. 72, 124–129.

Kumar, K., Vasanth, 2007. Optimum sorption isotherm by linear and non-linear methods for malachite green onto lemon peel. Dyes Pig. 74, 595–597.

Liew Abdullah, A.G., Mohd Salleh, M.A., Siti Mazlina, M.K., Megat Mohd Noor, M.J., Osman, M.R., Wagiran, R., Sobri, S., 2005. Azo dye removal by adsorption using waste biomass: sugarcane bagasse. Int. J. Eng. Technol. 2, 8–13.

Mittal, A., 2006. Adsorption kinetics of removal of a toxic dye, Malachite Green, from astewater by using hen feathers. J. Hazard. Mater. 133, 196–202.

Mondal, S., 2008. Methods of dye removal from dye house effluent-an overview. Environ. Eng. Sci. 25, 383–396.

Ponnusami, V., Vikram, S., Srivastava, S.N., 2008. Guava (Psidium guajava) leaf powder: Novel adsorbent for removal of methylene blue from aqueous solutions. J. Hazard. Mater. 152, 276–286.

Prahas, D., Kartika, Y., Indraswati, N., Ismadji, S., 2008. The use of activated carbon prepared from jackfruit (Artocarpus heterophyllus) peel waste for methylene blue removal. J. Environ. Prot. Sci. 2, 1–10.

Rao, V.V.B., Rao, S.R.M., 2006. Adsorption studies on treatment of textile dyeing industrial effluent by fly ash. Chem. Eng. J. 116, 77–84.

Sachdeva, S., Kumar, A., 2009. Preparation of nanoporous composite carbon membrane for separation of Rhodamine B dye. J. Membr. Sci. 329, 2–10.

Saeed, A., Sharif, M., Iqbal, M., 2010. application potential of grapefruit peel as dye sorbent: kinetics, equilibrium and mechanism of crystal violet adsorption. J. Hazard. Mater. 179, 564–572.

Sonawane, G.H., Shrivastava, V.S., 2009. Kinetics of decolourization of malachite green from aqueous medium by maize cob (Zea maize): an agricultural solid waste. Desalination 247, 430–441.

Tan, I.A.W., Ahmad, A.L., Hameed, B.H., 2008. Adsorption of basic dye on high- surface-area activated carbon prepared from coconut husk: equilibrium, kinetic and thermodynamic studies. J. Hazard. Mater. 154, 337–346.

Vimonses, V., Lei, S.M., Jin, B., Chowd, C.W.K., Saint, C., 2009. Kinetic study and equilibrium isotherm analysis of Congo Red adsorption by clay materials. Chem. Eng. J. 148, 354–364.

Zhang, J., LI, Y., Zhang, C., Jing, Y., 2008. Adsorption of malachite green from aqueous solution onto carbon prepared from Arundo donax root. J. Hazard. Mater. 150, 774–782.

Zonoozi, M.H., Moghaddam, M.R.A., Arami, M., 2009. Coagulation/flocculation of dye-containing solutions using polyaluminium chloride and alum. Water Sci. Technol. 59, 1343–1351.